Personalised Estimation of the Arterial Input Function for Improved Pharmacokinetic Modelling of Colorectal Cancer using dceMRI

Benjamin Irving[1], Lydia Tanner[1], Monica Enescu[1], Manav Bhushan[1], Esme J. Hill[3], Jamie Franklin[2], Ewan M. Anderson[2], Ricky A. Sharma[3], Julia A. Schnabel[1], and Sir Michael Brady[3]

[1] Institute of Biomedical Engineering, Department of Engineering Science, University of Oxford, Old Road Campus Research Building, Oxford, UK, OX3 7DQ
benjamin.irving@eng.ox.ac.uk
[2] Department of Radiology, Churchill Hospital, Old Road, Oxford, UK, OX3 7LE
[3] Department of Oncology, University of Oxford, Old Road Campus Research Building, Oxford, UK, OX3 7DQ

Abstract. dceMRI is becoming a key modality for tumour characterisation and monitoring of response to therapy, because of the ability to identify the underlying tumour physiology. Pharmacokinetic (PK) models relate the contrast enhancement seen in dceMRI to physiological parameters but require accurate measurement of the AIF, the time-dependant contrast concentration in blood plasma. In this study, a novel method is introduced that overcomes the challenges of direct AIF measurement, by automatically estimating the AIF from the tumour tissue. This approach was evaluated on synthetic data (10% noise) and achieved a relative error in K^{trans} and k_{ep} of $11.8 \pm 3.5\%$ and $25.7 \pm 4.7\%$, respectively, compared to $41 \pm 15\%$ and $60 \pm 32\%$ using a population model. The method improved the fit of the PK model to clinical colorectal cancer cases, was stable for independent regions in the tumour, and showed improved localisation of the PK parameters. This demonstrates that personalised AIF estimation can lead to more accurate PK modelling.

Keywords: pharmacokinetic model, arterial input function, dceMRI

1 Introduction

Dynamic contrast-enhanced magnetic resonance imaging (dceMRI) is becoming increasingly common for monitoring cancer response to therapy because of its ability to identify the underlying tissue physiology, such as microvasculature and capillary leakage, from tissue contrast agent (CA) uptake. During dceMRI acquisition, a bolus injection of CA is injected into a peripheral vein, which travels through the vascular system and leaks from the capillary network into the tissue extravascular-extracellular space (EES). Re-uptake and renal excretion then lowers the CA. This observed signal enhancement (S_e) can be modelled as

a convolution of an arterial input function (AIF) with a pharmacokinetic (PK) model to extract the physiological parameters of the tumour.

Accurate measurement of the AIF (the CA concentration in blood) is required for calculation of the AIF and PK convolution, however direct measurement from an artery is invasive and adds complexity to the dceMRI acquisition. The AIF can be measured directly from the dceMRI image by identification of an artery [1, 2], but the temporal resolution of dceMRI is generally too low to capture the initial AIF shape. Including an additional perfusion CT scan has been proposed but is often not feasible and adds radiation dose [3]. Population models of the AIF may be used as a substitute for direct AIF measurements [4, 2]. However, there is considerable inter- and intra-patient variability due to a number of physiological factors including heart rate, renal function and injection timing. We propose a novel approach to estimate the AIF from the tissue concentration curves, which does not require use of any additional measurements, modalities or reference regions. The method improves upon the initial population AIF estimate by jointly determining the optimal patient specific AIF and PK parameters from the tumour tissue region of interest (ROI). Unlike attempting to directly measure the AIF from an artery in dceMRI, a high temporal resolution is not required when estimating AIF from tissue concentration.

Some previous studies have developed methods to estimate patient specific AIFs. Liberman *et al.* [5] perform a search for optimal AIF parameters but require strict selection of voxels (brain grey and white matter); concentration curves with a visible proportion of plasma, which may not be present especially with a low temporal resolution; and find AIF and PK parameters independently – not accounting for interdependence. A similar method to ours is presented by Fluckiger *et al.* [6], by iteratively fitting the Tofts model [7] and an AIF model to eight representative curves derived from the tissue ROI. However, the method requires an AIF measurement to normalise the model; computationally intensive calculation of the convolution for each curve – therefore limited to eight curves; and an AIF model that requires 11 parameters to be fitted. The method we propose overcomes these limitations by including: knowledge of the population mean and variation to initialise and constrain the model, and an AIF model that requires fewer parameters. This allows an analytic solution to be found for the tissue concentration curve, which in turn speeds up the optimisation and allows the AIF to be optimised directly on at least 500 voxel tissue CA curves. No additional AIF measurements are required. Section 2 outlines our patient specific AIF estimation method to improve PK modelling, synthetic and clinical datasets are introduced in Section 3 and used for evaluation in Section 4.

2 Method

This section outlines our method to jointly determine the patient-specific AIF and PK parameters for a region of interest using dceMRI. As shown in Figure 1, the population AIF and tumour $S_e(t)$ curves are input into the model (Section 2.2). In this study, the Orton AIF [4] with Tofts PK model [7] (Section 2.1) are

used. However, other choices could be incorporated into this general framework. This model is fitted to each input $S_e(t)$ to derive the PK parameters. These parameters are then held fixed while a nonlinear fit determines the optimal AIF for the entire region. The updated AIF is used to generate an improved PK model fit. This is repeated using an alternating minimisation method until a final AIF and set of PK parameters for the region is found (Section 2.3).

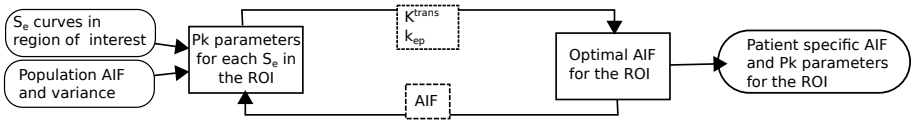

Fig. 1. The alternating minimisation framework for determination of patient specific AIF and improved pharmacokinetic parameter calculation

2.1 Tofts-Kety Model with Orton AIF

A common PK model is the Tofts-Kety two-compartment model where contrast is transferred between the blood plasma compartment and EES compartment [7]. Tissue concentration is described by $\frac{dC_e}{dt} = K^{trans}C_p - k_{ep}C_e$ with solution

$$C_e(t) = K^{trans}C_p(t) \otimes e^{-k_{ep}t} \tag{1}$$

where $\otimes$ is the convolution operator and change in tissue CA concentration (C_e) is determined by the CA concentration in blood plasma (C_p) and current C_e [7, 4]. As can be seen, C_e is dependant on accurate determination of the C_p (or AIF). This model can be fitted to concentration curves in dceMRI to derive physiological parameters (K^{trans}, k_{ep} and $v_e = K^{trans}/k_{ep}$). In this study we have made the assumption that the plasma fraction in the tumour is negligible ($v_p \approx 0$) [4]. The plasma fraction makes a contribution at the early vascular uptake stage which requires a high temporal resolution to detect. Bradley *et al* [8] also suggest that colorectal tumours have a low plasma fraction.

Orton *et al.* [4] provide a population model of the AIF that allows the Tofts model to be explicitly solved for C_e. The analytic solution to the Tofts-Kety model (Equation 1) with Orton AIF is:

$$\begin{aligned}
C_e(t) =& \frac{A_1A_2K^{trans}}{k_{ep}-m_2}\Big(f(t,m_2) + f(t,k_{ep})\Big(\frac{k_{ep}-m_2}{A_2} - 1\Big)\Big) \text{ for } 0 \le t \le t_B \\
C_e(t) =& \frac{A_1A_2K^{trans}}{k_{ep}-m_2}\Big(f(t_B,m_2)e^{-m_2(t-t_B)} \\
&+ \Big(\frac{k_{ep}-m_2}{A_2} - 1\Big)f(t_B,k_{ep})e^{-k_{ep}(t-t_B)}\Big) \text{ for } t > t_B \\
\text{with } f(t,\alpha) =& \frac{1}{\alpha}(1-e^{-\alpha t}) - \frac{1}{\alpha^2+m_1^2}(\alpha\cos(m_1t) + m_1\sin(m_1t) - \alpha e^{-\alpha t})
\end{aligned} \tag{2}$$

where A_1, A_1, m_1 and m_2 are the parameters of the AIF, K^{trans} and k_{ep} are the PK parameters of interest, and $t_B = 2\pi/m_1$. AIF offset (τ) is included in the AIF model to allow the bolus start time to be automatically determined such that $t = \hat{t} - \tau$ and $C_e(t) = 0$ for $t < 0$, where $\hat{t}$ is the measured time.

The relationship between tissue concentration $C_e(t)$ and observed signal enhancement $S_e(t)$ in dceMRI is nonlinear. $C_e(t)$ was converted to $S_e(t)$, using $S_e = \exp(-r_2 C(t) T_E) \frac{1-\exp(-P-Q)-\cos\alpha(\exp(-P)-\exp(-2P-Q))}{1-\exp(-P)-\cos\alpha(\exp(-P-Q)-\exp(-2P-Q))}$, where $P = T_R/T_{10}$ and $Q = r_1 C(t) T_R$, TR is the repetition time, TE is the echo time and r_1 and r_2 are known constants and α is the flip angle of the dceMRI image, from the Spoiled Gradient Recalled (SPGR) sequence model [9].

A key limitation of fitting Equation 2 is that globally scaling the AIF parameter A_1 over the entire region has the same result as scaling K^{trans} for each voxel. Therefore, A_1 is fixed as the population average to form an additional constraint on the AIF model. In our method, we use this analytic solution to derive the patient specific AIF for the ROI and voxelwise PK parameters.

2.2 Population AIF

In our AIF estimation method, the population AIF with variance is used to initialise and constrain the optimisation. Parker *et al.* [2] measured patient AIFs directly from high temporal-resolution dceMRIs of arteries of 67 scans of patients between 18 - 80 years. They used these measurements to develop a parametric function of AIF variation in a population. This model cannot be used to solve C_e analytically, and was used in our study to generate 1000 arterial input functions by sampling from the population distribution. These curves provide an estimate of the population mean and variance, and Orton *et al.*'s [4] model was fitted to each curve to generate the population mean and standard deviation for the model parameters: $A_1 = 2.65 \pm 0.18 mmol/l$, $A_2 = 1.51 \pm 0.68 mmol/l$, $m_1 = 22.40 \pm 0.73 min^{-1}$ and $m_2 = 0.23 \pm 0.46 min^{-1}$. These mean values are used as the initial AIF in order to derive a patient specific AIF.

2.3 Alternating Minimisation Method and Constraints

The previous sections outline the AIF and PK models that are used in our patient specific AIF estimation method. Optimal parameters for both the models (described in Section 2.1) are found from the dceMRI ROI in an alternating minimisation method. The alternating minimisation method is initialised using the population AIF, and the model is fitted to each dceMRI S_e curve to derive the PK parameters using the 'trust-region-reflective' method for non-linear least squares curve fitting. In this initial step, PK parameters are derived for each voxel. These PK parameters are used to fit the same model over the entire region to determine the optimal AIF parameters, while keeping the PK parameters fixed. This new AIF model is then used to improve the individual PK parameter estimation for each voxel. This is repeated until convergence (shown in Figure 1).

Bounds are set on the AIF parameters to be within 4 standard deviations of the population average – representing 99.99% of the population – and a bound of $v_e \leq 1$. The lumen may be included in the ROI due to movement from peristalsis. To exclude these voxels, voxels that show no enhancement at temporal postions after initial enhancement are excluded.

Therefore, our model is able to obtain patient specific AIF and PK parameters without additional blood sampling, scans or the assumption of a population AIF. This method was evaluated on synthetic and clinical datasets.

3 Materials

3.1 Synthetic Images

Synthetic data was used to evaluate the method by generating signal enhancement (S_e) curves from known PK parameters and AIFs. These known PK parameters and AIFs were compared to the parameters derived by our method on the synthetic data. 30 synthetic cases were generated, each consisting 500 signal enhancement curves. These were generated with 0%, 5% and 10% added noise. Each of the 500 voxels consisted of 29 temporal positions with a temporal resolution of 9.5s – consistent with the clinical data in this Section.

Each case consisting of 500 voxels was generated from the same sampled AIF and each voxel from a set of PK parameters. AIFs were derived for each case by sampling from a Gaussian distribution over the means and standard deviations of the Orton AIF parameters. This AIF was kept fixed for each of the 10 datasets while generating 500 K_{trans} and k_{ep} pair to calculate individual signal enhancement curves. K_{trans} was derived from a uniform distribution on the interval [0,2] and v_e was derived from [0.4,1], $k_{ep} = K_{trans}/v_e$, and the offset was sampled from [0, 0.5] minutes. These parameters and the AIF values were then used with the Tofts and Orton AIF model to generate the 500 signal enhancement curves. Noise was added to each temporal position of each voxel by sampling from a Gaussian distribution with standard deviation equal to 0%, 5% and 10% of the mean enhancement of the curve. Example synthetic S_e curves are shown in Figure 5c) and Figure 5f).

3.2 dceMRI Colorectal Cancer Cases

Six dceMRI images were acquired as part of a phase 0/1 drug trial with hypofractionated radiotherapy in patients with colorectal cancer. Pre- and post-treatment image sequences were acquired. A 3T GE scanner was used to acquire the dceMRI images with the LAVA protocol and spoiled gradient echo sequence. Images with dimensions 512x512x52x29 were acquired with voxel size of 0.78x0.78x2.00mm, and a temporal resolution of 9.5s. ProHance (Gadoteriol) contrast was injected at a rate of 3 ml/sec, 0.1 mmol/kg body weight. Colorectal tumours were delineated by a clinician on T2 weighted images and registered to the dceMRI image. Flip-angle images were not available and a uniform T_{10} map of 1 was assumed. Figure 2 shows a cross section of a tumour ROI before and after CA enhancement. K^{trans} maps of this ROI are shown later in Figure 7.

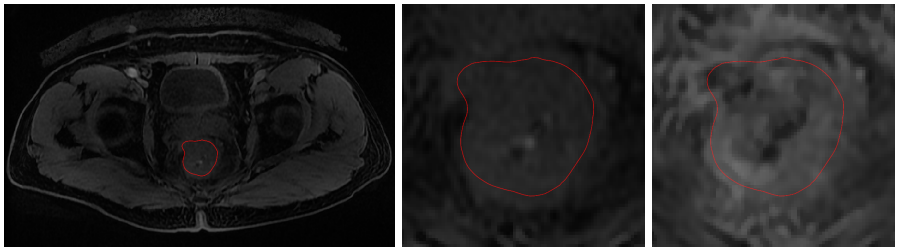

(a) (b) (c)

Fig. 2. dceMRI slice through centre of colorectal tumour for Patient 1, with b) zoomed in ROI before contrast (0s) and c) after contrast enhancement (276s)

4 Results

4.1 Results using Simulated Data

Our patient specific AIF estimation method was evaluated on each of the 10 sets of data at each noise level of 0%, 5% and 10%. The alternating minimisation method was run for 100 iterations to determine the patient specific PK parameters and AIF. Figure 3 shows the normalised residual 2-norm error in the fit of the model to the signal enhancement curves for a) the first on synthetic data and b) the on clinical data with the standard deviation representing the variation between the cases. The first iteration is the fit using a population AIF and the remaining iterations show the error as a proportion of this initial fit. As expected, there is a considerable improvement in fit of the pharmacokinetic model to the signal enhancement curves by finding a patient specific AIF. Synthetic data at 10% noise and clinical data achieved fits with errors of $12.6 \pm 12.8\%$ and $27.8 \pm 16.0\%$, respectively, of the initial population model fit.

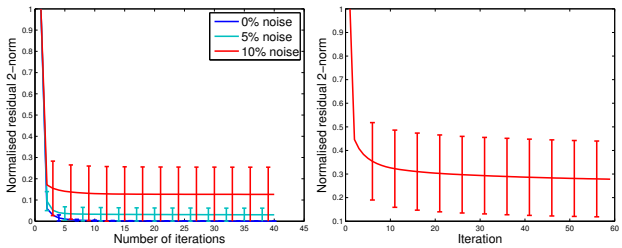

(a) Synthetic cases (b) Clinical cases

Fig. 3. Normalised residual 2-norm error for each iteration of our AIF estimation method a) synthic cases with 0%, 5% and 10% added Gaussian noise b) clinical cases. These results are normalised by the error using the population AIF (first iteration)

The relative error and correlation between the derived PK parameters and the known PK parameters (used to generated the synthetic data) are shown in Figure 4. Our patient specific AIF method achieves a very high correlation between the 'truth' and derived PK parameters –important for analysis of heterogeneity in tumours. The accuracy of the PK parameters is also considerably improved compared to the PK parameters derived using a population AIF. K^{trans} relative error with 10% noise was $11.8 \pm 3.5\%$ (from $41 \pm 15\%$) and k_{ep} error of 25.7 ± 4.7 (from $60 \pm 32\%$). This demonstrates the benefit of our method and the importance of determining a patient specific AIF for PK parameter calculations. Noise impacts the accuracy of derived PK parameters (particularly k_{ep}) but are still considerably better than the population AIF derived values even without noise. There is a small error in K^{trans} even without added noise due to the assumption of a population A_1 parameter.

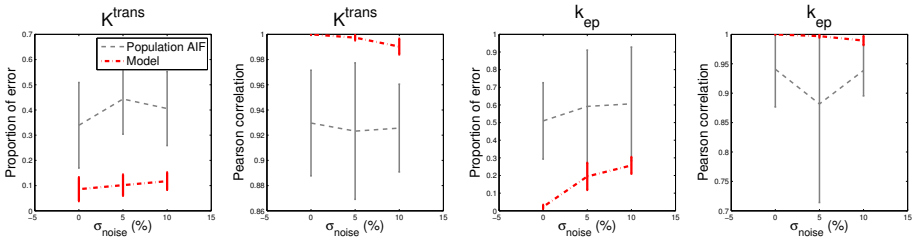

Fig. 4. Error and correlation of K^{trans} and k_{ep} using the population average and patient specific AIF on synthetic cases. The dashed grey lines show the calculated K^{trans} and k_{ep} using the population AIF while the red lines show the PK parameters calculated using the derived patient specific AIF. The x-axis is the standard deviation of the Gaussian noise in the synthetic data and the error bars show the standard deviation of the relative error in the 10 datasets.

Two examples of the AIF optimisation are shown in Figure 5a-c) and Figure 5d-f). The derived patient specific AIFs matched the known AIFs closely. In Figure 5a-c), the PK parameters used to generate the synthetic curve were K^{trans}=0.608 and k_{ep}=0.615. Parameters derived using the population AIF were less accurate (0.712 and 0.864) compared to those derived using the patient specific AIF (0.548 and 0.615). In this example, there is little offset or bolus peak difference between the population AIF and 'true' AIF. However, just the increased tail of the AIF has a considerable impact on the concentration curve fit and accuracy of PK parameters, particularly k_{ep}.

4.2 Results using Colorectal dceMRI

Our patient specific AIF method was applied to six clinical cases. Figure 3b) shows that a considerably improved fit to the SE curves in the scan is achieved using a patient specific AIF ($< 30\%$ of the original error). Therefore, the patient

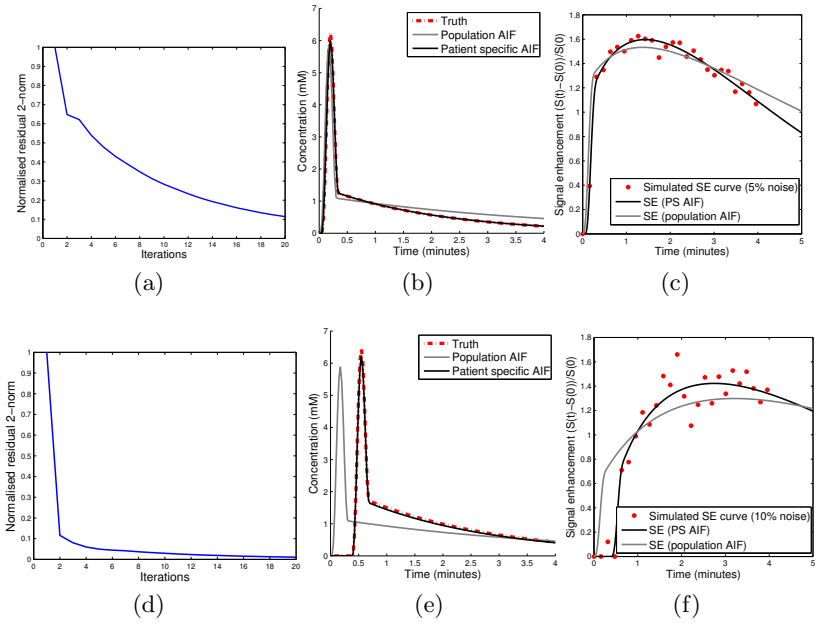

Fig. 5. Patient specific AIF compared to the known AIF for two synthetic cases a-c and d-f. a) and d) show the error between the known AIF and the estimated AIF over the first 20 iterations of the algorithm. b) and e) compare the population AIF and the derived patient specfic AIF to the known AIF used to generate the synthetic data (dashed curve). c) and e) show one example of the 500 signal enhancement curves in a case that are used to derive the parameters, where grey is the fitted curve using the population AIF and black is the fitted curve using our patient specific AIF.

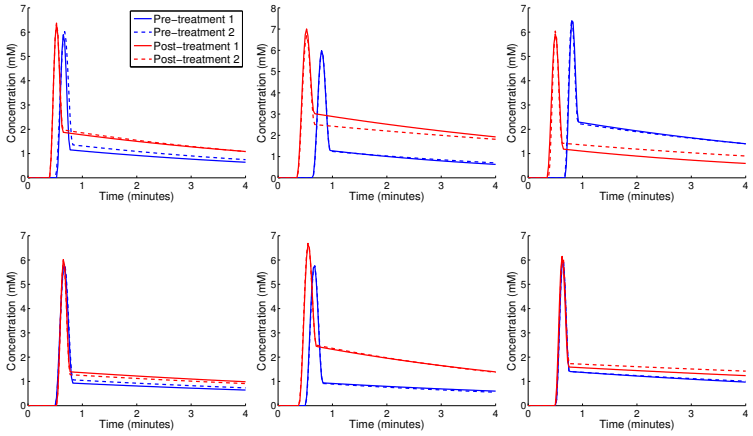

Fig. 6. Pre- and post-treatment AIFs found for 6 clinical colorectal cancer cases. Two AIFs were generated using independent regions in the tumour in each image.

specific AIF results in a PK model that is more representative of tumour signal enhancement. Figure 6 shows AIF curves generated for pre-treatment (gray) and post-treatment (black) for the centre tumour slice (solid line) and the following slice (dashed lines) for 6 cases. The similarity between the AIF derived from neighbouring slices shows that the model is stable when optimised on independent regions of the tumour. Interestingly, the AIFs show a trend of having a larger 'tail' for post therapy images. Therefore, as well as improving the accuracy of PK parameter estimation, AIF shape may have diagnostic value. Figure 7 shows example K^{trans} maps for the centre slice of the tumour ROI for the pre and post radiotherapy using both the population and derived patient specific AIF. Increased localisation and defined focal points of activity are shown with use of the correct offset and patient specific AIF.

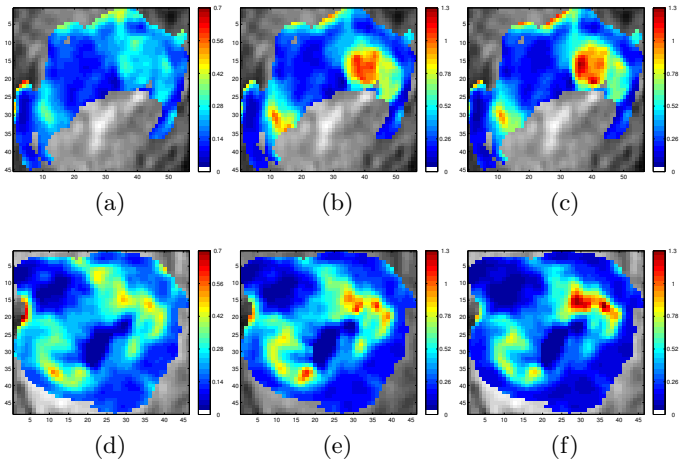

Fig. 7. K^{trans} maps for a cross-section of the tumour ROI (color) with image background for Patient 1. a)-c) show pre-radiotherapy and d-f) post radiotherapy. a) and d) Population AIFs with an incorrect offset (30s error), b) and e) Population AIFs with corrected offset and c) and f) patient specific AIFs derived using our model.

5 Discussion and Conclusions

PK parameter calculation in dceMRI requires accurate measurement of the AIF. This is often not possible and a population AIF is used instead, which results in inaccuracies. In this study, a novel method to obtain a patient specific AIF from the population model and tissue ROI is introduced. Unlike previous methods, our method does not require additional scans, direct measurements or identification of an artery. The optimisation is also applied directly to a large number of signal enhancement curves in the ROI, making the fit robust and adaptable.

This method considerably improves the PK model fit compared to the population AIF for both synthetic and clinical dceMRI cases, leading to more accurate PK parameters. In synthetic data, the K^{trans} relative error with 10% noise was $11.8 \pm 3.5\%$ (from $41 \pm 15\%$) and k_{ep} error of 25.7 ± 4.7 (from $60 \pm 32\%$). In clinical cases the AIF produces robust results for independent regions in the tumour. Future work will include: incorporation of motion correction into the method and use of this patient specific AIF model to better estimate patient response to therapy. There is also potential to compare the personalised AIF to direct AIF measurements from high temporal resolution scans of an artery, and also examine the effect of temporal resolution on AIF estimation.

Acknowledgements: This work was supported by the CRUK/EPSRC Oxford Cancer Imaging Centre. We thank Prof. Fergus Gleeson for the dceMRI dataset.

References

1. Rijpkema, M., Kaanders, J.H., Joosten, F.B., van der Kogel, A.J., Heerschap, A.: Method for quantitative mapping of dynamic MRI contrast agent uptake in human tumors. Magn Reson Imaging 14, 457–63 (2001)
2. Parker, G., Roberts, C., Macdonald, A., Buonaccorsi, G., Cheung, S., Buckley, D., Jackson, A., Watson, Y., Davies, K., Jayson, G.: Experimentally-derived functional form for a population-averaged high-temporal-resolution arterial input function for dynamic contrast-enhanced MRI. Magn Reson Med 56, 993–1000 (2006)
3. Enescu, M., Bhushan, M., Hill, E.J., Franklin, J., Anderson, E.M., Sharma, R.A., Schnabel, J.A.: pCT derived arterial input function for improved pharmacokinetic analysis of longitudinal dceMRI for colorectal cancer. SPIE p. 86690L (2013)
4. Orton, M.R., D'Arcy, J.a., Walker-Samuel, S., Hawkes, D.J., Atkinson, D., Collins, D.J., Leach, M.O.: Computationally efficient vascular input function models for quantitative kinetic modelling using DCE-MRI. Phys Med Biol 53, 1225–39 (2008)
5. Liberman, G., Louzoun, Y., Colliot, O., Ben Bashat, D.: T1 Mapping, AIF and Pharmacokinetic Parameter Extraction from Dynamic Contrast Enhancement MRI Data. In: Liu, T., Shen, D., Ibanez, L., Tao, X. (eds.) Multimodal Brain Image Analysis, LNCS, vol. 7012, pp. 76–83. Springer, Heidelberg (2011)
6. Fluckiger, J.U., Schabel, M.C., DiBella, E.V.R.: Model-based blind estimation of kinetic parameters in dynamic contrast enhanced (DCE)-MRI. Magn Reson Med 62, 1477–1486 (2009)
7. Tofts, P.S., Brix, G., Buckley, D.L., Evelhoch, J.L., Henderson, E., Knopp, M.V., Larsson, H.B.W., Lee, T.Y., Mayr, N.A., Parker, Others: Estimating kinetic parameters from dynamic contrast-enhanced T 1-weighted MRI of a diffusable tracer: standardized quantities and symbols. Magn Reson Imaging 10, 223–232 (1999)
8. Bradley, D.P., Tessier, J.L., Checkley, D., Kuribayashi, H., Waterton, J.C., Kendrew, J., Wedge, S.R.: Effects of AZD2171 and vandetanib (ZD6474, Zactima) on haemodynamic variables in an SW620 human colon tumour model : an investigation using dynamic contrast-enhanced MRI and the rapid clearance blood pool contrast agent, 20, 42–52 (2008)
9. Tofts, P.S., Kermode, A.G.: Measurement of the blood-brain barrier permeability and leakage space using dynamic MR imaging. 1. Fundamental concepts. Magn Reson Med 17, 357–367 (1991)